



Get Clarity On Generics

Cost-Effective CT & MRI Contrast Agents

**FRESENIUS
KABI**

[WATCH VIDEO](#)

AJNR

This information is current as
of August 18, 2025.

DWI-Based Radiomics Predicts the Functional Outcome of Endovascular Treatment in Acute Basilar Artery Occlusion

X. Zhang, J. Miao, J. Yang, C. Liu, J. Huang, J. Song, D.
Xie, C. Yue, W. Kong, J. Hu, W. Luo, S. Liu, F. Li and W.
Zi

AJNR Am J Neuroradiol 2023, 44 (5) 536-542

doi: <https://doi.org/10.3174/ajnr.A7851>

<http://www.ajnr.org/content/44/5/536>

DWI-Based Radiomics Predicts the Functional Outcome of Endovascular Treatment in Acute Basilar Artery Occlusion

 X. Zhang,  J. Miao,  J. Yang,  C. Liu,  J. Huang,  J. Song,  D. Xie,  C. Yue,  W. Kong,  J. Hu,  W. Luo,  S. Liu,  F. Li, and  W. Zi



ABSTRACT

BACKGROUND AND PURPOSE: Endovascular treatment is a reference treatment for acute basilar artery occlusion (ABAO). However, no established and specific methods are available for the preoperative screening of patients with ABAO suitable for endovascular treatment. This study explores the potential value of DWI-based radiomics in predicting the functional outcomes of endovascular treatment in ABAO.

MATERIALS AND METHODS: Patients with ABAO treated with endovascular treatment from the BASILAR registry (91 patients in the training cohort) and the hospitals in the Northwest of China (31 patients for the external testing cohort) were included in this study. The Mann-Whitney *U* test, random forests algorithm, and least absolute shrinkage and selection operator were used to reduce the feature dimension. A machine learning model was developed on the basis of the training cohort to predict the prognosis of endovascular treatment. The performance of the model was evaluated on the independent external testing cohort.

RESULTS: A subset of radiomics features ($n = 6$) was used to predict the functional outcomes in patients with ABAO. The areas under the receiver operating characteristic curve of the radiomics model were 0.870 and 0.781 in the training cohort and testing cohort, respectively. The accuracy of the radiomics model was 77.4%, with a sensitivity of 78.9%, specificity of 75%, positive predictive value of 83.3%, and negative predictive value of 69.2% in the testing cohort.

CONCLUSIONS: DWI-based radiomics can predict the prognosis of endovascular treatment in patients with ABAO, hence allowing a potentially better selection of patients who are most likely to benefit from this treatment.

ABBREVIATIONS: ABAO = acute basilar artery occlusion; AUC = area under the receiver operating characteristic curve; CAPS = critical area perfusion score; EVT = endovascular treatment; LASSO = least absolute shrinkage and selection operator; ML = machine learning; pc = posterior circulation; pcASCO = posterior circulation ASPECTS-Collaterals score; RF = radiomics feature

Acute basilar artery occlusion (ABAO) is a rare but very aggressive subtype of ischemic stroke with high rates of mortality and disability, accounting for approximately 1% of all ischemic strokes and

5%–10% of large-vessel occlusion strokes.^{1–3} Recently, 2 prospective multicenter randomized clinical trials (the Basilar Artery Occlusion Chinese Endovascular trial [BAOCHE]⁴ and the Endovascular Treatment for Acute Basilar-Artery Occlusion trial [ATTENTION⁵]) and our previous the EVT for Acute Basilar Artery Occlusion Study (BASILAR) registry study⁶ indicated that endovascular treatment (EVT) for patients with ABAO resulted in better functional outcomes than the best medical treatment. However, current evaluation methods for preoperative images of ABAO are limited compared with anterior circulation ischemic stroke.

Previous studies have identified several indicators and scoring systems that predict the prognosis of patients with ABAO, such as ASPECTS, the combined collateral status and ASPECTS scores (PCASCO), and infarct volume. However, their performance in predicting outcomes is not satisfactory. This issue may be explained by the posterior fossa radiologic particularities and the anatomic differences in the posterior circulation. Accurate and specific preoperative assessment and selection are key to determining EVT prognosis. Thus, there is an urgent need to develop an effective method for assessing the benefits of EVT in patients with ABAO.

Received December 27, 2022; accepted after revision March 15, 2023.

From the Department of Neurology (X.Z., J.M., J.Y., C.L., J.H., J.S., D.X., C.Y., W.K., J.H., W.L., S.L., F.L., W.Z.), Xinqiao Hospital and The Second Affiliated Hospital, Army Medical University (Third Military Medical University), Chongqing, China; Department of Neurology (X.Z.), The Affiliated Hospital of Northwest University Xi'an No.3 Hospital, Xian, China; and Department of Neurology (J.M.), Xianyang Hospital of Yan'an University, Xianyang, China.

Xiao Zhang, Jian Miao, and Jie Yang contributed equally as co-first authors.

Both Wenjie Zi and Fengli Li are co-senior authors.

This work was supported by the National Natural Science Foundation of China (No. 82071323), and the Chongqing Natural Science Foundation (cstc2020cyj-msxmX0926).

Please address correspondence to Wenjie Zi, MD, Department of Neurology, Xinqiao Hospital and The Second Affiliated Hospital, Army Medical University (Third Military Medical University), No. 183 Xinqiao Main St, Shapingba District, Chongqing 400037, China; e-mail: ziwenjie1981@163.com

 Indicates open access to non-subscribers at www.ajnr.org

 Indicates article with online supplemental data.

<http://dx.doi.org/10.3174/ajnr.A7851>

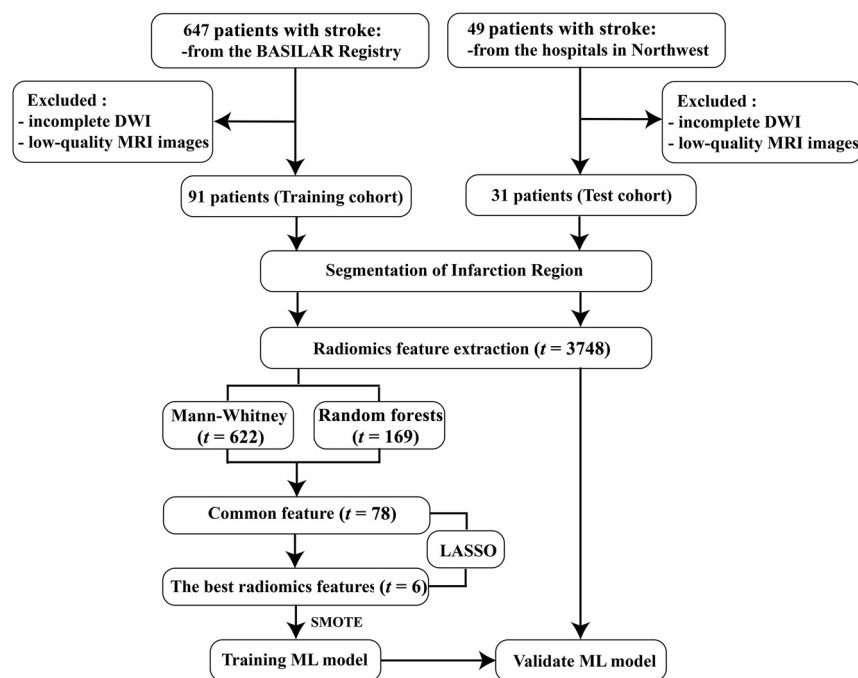


FIG 1. Flowchart of research patients and process. SMOTE indicates synthetic minority oversampling technique.

The concept of radiomics has recently been applied in many fields to quantitatively assess lesions by extracting large amounts of high-dimensional imaging information from conventional images, helping to reflect lesion characteristics beyond morphologic features and adding value to MR imaging guides for early stroke treatment.⁷ In contrast to measuring features, such as the volume and signal intensity of infarct regions of brain tissue, radiomics is characterized by the ability to detect many-but-subtle changes in the area of interest that are not recognizable to the human eye.⁸ The fusion of deeply mined imaging information with machine learning (ML) techniques can provide valuable diagnostic, prognostic, or predictive information for the treatment of clinical diseases.⁹ Recently, a novel prognostic evaluation consisting of radiomics and ML has been proposed to predict the time to onset¹⁰ and prognosis^{11,12} of acute ischemic stroke in the anterior circulation. These high-dimensional features exhibited superior diagnostic advantages and ability, with good sensitivity and specificity in predicting prognosis and treatment strategies.¹³⁻¹⁵ To our knowledge, no other study based on radiomics has predicted the functional outcome of patients with ABAO on presurgical DWI.

Therefore, our study aimed to investigate the value of DWI-based radiomics in predicting the functional outcomes of EVT for ABAO. Additionally, we tested the diagnostic performance of the model in an independent external testing cohort.

MATERIALS AND METHODS

Ethics Statements

Permission was obtained from the ethics committee of the Xinqiao Hospital (Second Affiliated Hospital), Army Medical

University Board (2013-yandi-08701), and written informed consent was obtained from all patients or their legal representatives.⁶ The research of clinical features and imaging material was decided by the group. The BASILAR study was registered with the Chinese Clinical Trial Registry (<http://www.chictr.org.cn>; ChiCTR1800014759). The study has been conducted according to the principles expressed in the Declaration of Helsinki.

Participants

The training cohort used the BASILAR registry, a multicenter, observational study including 647 consecutive patients with ABAO who underwent EVT from January 2014 to May 2019 in 47 senior stroke centers across 15 provinces in China. The test cohort enrolled patients with ABAO from Xianyang Hospital of Yan'an University and The Affiliated Hospital of Northwest University between April 2018 and June 2022 (Fig 1). We have verified that there are

no overlapping patients in the 2 cohorts. The study followed the Strengthening the Reporting of Observational Studies in Epidemiology (STROBE) reporting guideline. We included only patients who underwent both NCCT and DWI before EVT. Patients were excluded in case of low-quality images (eg, motion artifacts or metal artifacts). The training cohort was used to select relevant radiomics features (RFs) and build a predictive ML model; then, we used the testing cohort to evaluate the accuracy of the predictive model. Because patients with ABAO have a worse prognosis than those with anterior circulation stroke, patients with an mRS of ≤ 3 on the 90th day after EVT were defined as having a favorable functional outcome, whereas those with an mRS > 3 showed an unfavorable functional outcome.

Segmentation of the Infarct Region

Infarct regions were manually segmented with 3D Slicer (Version 4.11; <http://www.slicer.org>).¹⁶ Additionally, we viewed the corresponding ADC image for guidance. The ROI (infarct region) of segmentation was based on the weight of the posterior circulation (pc)-ASPECTS. Two points each are subtracted for high signal in the right or left pons or midbrain, independently, and 1 point each is subtracted for high signal in any part of the cerebellum, thalamus, or occipital cortex.¹⁷ The ROI (infarct region) in both cohorts has manually segmented the images by an experienced neuroradiologist (reader A, blinded to the eventual diagnosis) along the intraparenchymal regions of the high-signal contour on each transverse section (Fig 2A, -B). With reference to a guideline of reliability research,¹⁸ we selected all patients for assessing the interoperator agreement of feature extraction. A senior neuroradiologist re-segmented the images of all patients (reader B, blinded to the eventual diagnosis). Both neuroradiologists were

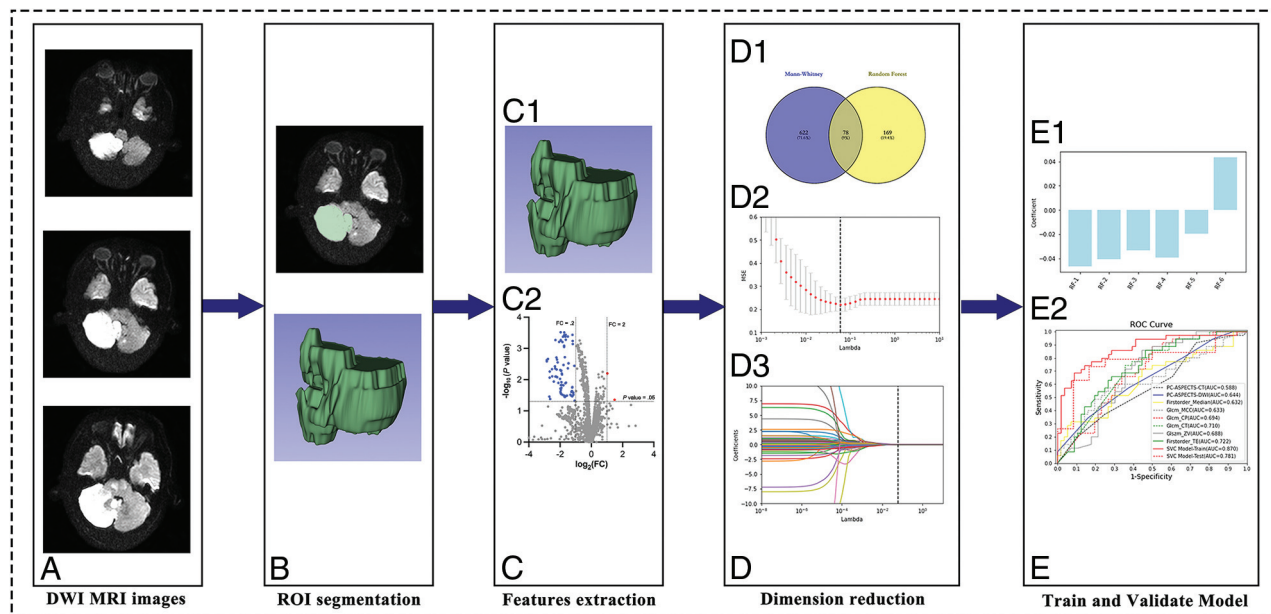


FIG 2. The radiomics analysis schematic. A, DWI. B, ROI. C1, ROI in 3D space. C2, Overall distribution of different RFs. The different features were analyzed between the 2 groups using a volcano plot. Red dots represent positive correlations with good outcomes, whereas blue dots represent negative correlations. FC indicates fold change. D1, Venn diagram (Mann-Whitney *U* test and random forests). D2, Radiomics feature determination using the LASSO regression with 5-fold cross-validation. The smallest mean squared error (MSE) corresponds to the number of horizontal coordinates for the best λ value. D3, LASSO coefficient profiles of the 78 RFs. The best RFs with nonzero coefficients at a λ value of 0.06 were selected. E1, The selected RFs and their coefficients. A coefficient of >0 means that the characteristic is positively correlated with the outcome, whereas a coefficient of <0 means that it is negatively correlated with the outcome. E2, Receiver operating characteristic curve results of the best RFs from different feature classifications compared with ASPECTS from conventional imaging.

Table 1: Feature classification

RF Class	No. of RFs
Set 1: First-order statistics	36
Set 2: Shape-based	28
Set 3: Textural features	
Gray-level co-occurrence matrix	48
Gray-level dependence matrix	28
Gray-level run length matrix	32
Gray-level size zone matrix	32
Neighboring gray tone difference matrix	10
Image filter	
LoG	930
Wavelet	1488
Square	186
Square root	186
Logarithm	186
Exponential	186
Gradient	186
Lbp2D	186

Note:—LoG indicates laplacian of gaussian; Lbp2D, local binary pattern 2D.

blinded to the final diagnosis. Interobserver repeatability of lesion segmentation was assessed by calculating the κ coefficients of the extracted RFs ($\kappa = 0.97$, 95% CI, 0.894–0.980). Good agreement was defined as RFs with κ coefficients of >0.75 .

RF Extraction

Substantial RFs were automatically extracted from the diffusion-weighted images with the use of pyradiomics (Version: latest; <https://pyradiomics.readthedocs.io/en/latest/>), including first-order statistics, shape-based features, and textural features (Table 1):

Set 1: First-order statistics can quantify the intensity characteristics by calculating all voxels within the infarct region.

Set 2: This set included shape features, eg, the infarct length, surface, and volume.

Set 3: Textural features quantify textural heterogeneity within the infarct region.

Further higher-order features were found by applying filters to native DWI (Table 1). A detailed definition of RFs can be obtained from the pyradiomics Web site (<https://pyradiomics.readthedocs.io/en/latest/>).

RF Selection and Classification

Before building a prognostic prediction model for ABAO, we used the Mann-Whitney *U* test and the random forests algorithm to screen relevant features in the training cohort (Fig 1). On the basis of 5-fold cross-validation, the least absolute shrinkage and selection operator (LASSO) regression model selected the optimal features and extracted those with nonzero coefficients. RFs were tested for collinearity using the collinearity diagnosis in the linear regression analysis, and features with a variance inflation factor of >10 were excluded. To eliminate the biases of class in the negative and positive distributions, radiomics data adopted the synthetic minority oversampling technique, which can potentially improve the efficacy of the model.¹⁹ The predictive model was based on a support vector machine classifier, and its best parameters were evaluated by the grid search cross-validation method in the training cohort. A radiomics model was constructed on the training cohort and then validated on the testing cohort. The predictive performance of the radiomics model was assessed using accuracy, specificity, sensitivity, negative predictive value, positive predictive value, and the area under the receiver operating

characteristic curve (AUC). The dimension reduction of the radiomics features and the development of the radiomics models were implemented in scikit-learn (Version 1.0.2; <https://scikit-learn.org/stable/>).

Clinical Data Collection and Statistical Analysis

All neuroimaging scores were evaluated using an imaging core laboratory. Continuous variables such as demographic data and clinical characteristics were compared using the independent samples *t* test or Mann-Whitney *U* test. Categorical variables were tested using the χ^2 test or Fisher exact test. Descriptive statistics are expressed as mean (SD) or median (interquartile range) for continuous variables and as frequency (percentage) for categorical variables. The *P* values for all tests were 2-tailed. All tests were considered statistically significant at *P* < .05. We excluded patients with missing essential data from this analysis; thus, there was no need for imputation. All of the aforementioned analyses were implemented using the Python platform with an in-house code (Version 3.9; Guido van Rossum) and SPSS statistical analysis software (Version 26.0; IBM).

RESULTS

Patient Characteristics

All patients completed the 90 days of follow-up and were included in the final analysis. The Online Supplemental Data present the differences in the baseline characteristics of the patients in the training cohort by favorable and unfavorable functional outcomes. Except for the baseline NIHSS score, pc-ASPECTS (DWI), infarct volume, expanded TICI, and recanalization time, no other characteristics were significantly different (*P* < .05).

Among the patients with different clinical outcomes at 90 days, those with favorable functional outcomes had a lower initial NIHSS score (15 [range, 6–23] versus 28 [range, 20–32], *P* < .001) than those with unfavorable functional outcomes before EVT. In both groups, the DWI ASPECTS was slightly lower than the NCCT ASPECTS (7 [range, 6–8] versus 6 [range, 5–7]; *P* = .019 and 8 [range, 7–9] versus 8 [range, 6–9]; *P* = .15, respectively). Compared with patients with unfavorable functional outcomes, patients with favorable functional outcomes had lower baseline mean infarct volumes in the pons and midbrain (1.2 [SD, 0.9] versus 2.3 [SD, 1.8]; *P* = .001; Online Supplemental Data). Patients with favorable functional outcomes had higher rates of substantial reperfusion (expanded TICI score) on the final angiogram than those in the unfavorable functional outcomes group (*P* = .001). The baseline characteristics of the patients in the testing cohort are shown in the Online Supplemental Data.

Selecting the Best RFs

We found good agreement between the 2 readers after assessing the interobserver reliability of morphology measurements using κ coefficients (κ = 0.97; 95% CI, 0.894–0.980). According to the pc-ASPECTS regions, many RFs were automatically extracted from the infarct regions using pyradiomics. A total of 3748 RFs were extracted from the DWI, including 14 shape-based features, 18 first-order statistical parameters, 24 gray-level co-occurrence matrix indexes, 14 gray-level dependence matrix features, 16 gray-level run length matrix parameters, 16 gray-level size zone

matrixes, and 5 neighboring gray tone difference matrix features. Further higher-order features were extracted after applying the filters to the DWI (Table 1).

The volcano plot demonstrates the distribution of different RFs between the 2 groups (Fig 2C2), according to the criteria of \log_2 fold change ≥ 1 and *P* < .05. The results showed that features marked in red represent up-regulation, features marked in blue represent down-regulation, and features marked in gray represent no significant difference between the 2 groups. The 3748 features were preliminarily screened using 2 algorithms: the *t* test and random forests (Fig 2D1). Most of the 78 features preliminarily screened by these 2 algorithms were all related to the brainstem infarct region (Online Supplemental Data). The LASSO regression model (Fig 2D2, -D3) was further used to reduce the dimensionality of the RFs, resulting in 6 DWI features to build the radiomics models. The following characteristic was positively associated with a favorable functional outcome: wavelet-HLL_glcM_MCC. The remaining 5 characteristics were negatively associated with favorable functional outcomes: 1) brainstem-log-sigma-1-0-mm-3D_glcM_ClusterProminence; 2) brainstem-log-sigma-2-0-mm-3D_glcM_ClusterTendency; 3) brainstem-wavelet-LHH_glszm_ZoneVariance; 4) brainstem-wavelet-HHL_firstorder_Median; and 5) brainstem-lbp-2D_firstorder_TotalEnergy (Fig 2E1).

Predictive Role of Traditional Imaging Indicators and RFs in Prognosis

The traditional imaging and radiomics indicators related to prognosis are shown in Fig 3. Among traditional imaging indicators, DWI ASPECTS (AUC = 0.644; 95% CI, 0.528–0.760) had a slightly higher predictive value than CT ASPECTS (AUC = 0.588; 95% CI, 0.469–0.708) for favorable functional outcome.²⁰ The AUC is 0.701 (95% CI, 0.609–0.80) for the infarct volume in the pons and midbrain.

The predictive accuracy of RFs was higher than that of conventional imaging metrics, such as wavelet-HLL_glcM_MCC (AUC = 0.633; 95% CI, 0.525–0.731); brainstem-lbp-2D_firstorder_TotalEnergy (AUC = 0.722; 95% CI, 0.619–0.811); brainstem-log-sigma-1-0-mm-3D_glcM_ClusterProminence (AUC = 0.694; 95% CI, 0.588–0.786); brainstem-log-sigma-2-0-mm-3D_glcM_ClusterTendency (AUC = 0.710; 95% CI, 0.605–0.800); brainstem-wavelet-HHL_firstorder_Median (AUC = 0.632; 95% CI, 0.524–0.731); and brainstem-wavelet-LHH_glszm_ZoneVariance (AUC = 0.688; 95% CI, 0.582–0.781). After the covariance test was performed for the radiomics indicators, all tolerances were >0.1, and all variance inflation factors were <10; thus, it was thought that there was no covariance among the variables (Online Supplemental Data). Figure 4 shows 2 examples of segmentations from patients with ABAO with favorable (case 2) and unfavorable (case 1) outcomes.

External Validation of the Prognostic Prediction Models

The radiomics model based on the 7 selected RFs accurately predicted different prognoses after EVT in the independent testing cohort. It had an overall accuracy of 77.4%, a sensitivity of 78.9%, a specificity of 75%, a positive predictive value of 83.3%, and a negative predictive value of 69.2%. In the training cohort,

the AUC of the radiomics model was 0.870 (95% CI, 0.784–0.932). In the testing cohort, the AUC of the radiomics model was 0.781 (95% CI, 0.596–0.908). Detailed information is provided in Table 2.

DISCUSSION

To our best knowledge, this is the first multicenter MR imaging study to investigate the value of DWI-based radiomics in predicting

the functional outcome of EVT in ABAO.²¹ We aimed to predict a favorable prognosis for patients with ABAO based on the RFs obtained in the infarct region on preoperative DWI. One of the 6 selected RFs was positively associated with a favorable prognosis: the maximal correlation coefficient. Five of the 6 selected RFs were negatively associated with a favorable prognosis: cluster prominence, cluster tendency, zone variance, median, and total energy. Median and total energy are first-order features describing

the distribution of voxel intensities within the infarct region (image gray-scale values). Cluster prominence, cluster tendency, and maximal correlation coefficient belong to the gray-level co-occurrence matrix feature, which is used to describe the spatial relationship between the gray-scale values of neighboring voxels in the infarct region. Zone variance is classified as a gray size area matrix feature that describes the spatial distribution of neighboring voxels with similar gray-scale values in the infarct region. A more detailed description of the radiomics features is shown on the Web site <https://pyradiomics.readthedocs.io/en/latest/>. The formula and method of calculating the RFs are shown in the Online Supplemental Data.

Whether EVT will likely lead to a favorable prognosis for patients with ABAO is, in our view, an important piece of information that can help doctors make applicable decisions about the transport, triage, and treatment of patients, particularly when the risks of performing EVT are considered. The aims of prognostic prediction for patients before EVT are to exclude those for whom intervention may be futile and to evaluate which patients may benefit. Patients in whom the possibility of a favorable prognosis with EVT is very high and who may have a lower risk of bleeding may benefit from direct transport to EVT. Patients in whom the possibility of a favorable prognosis with EVT is very low and who may have difficult or risky endovascular access could be given conservative drug treatment and observed for improvement. These considerations can also be

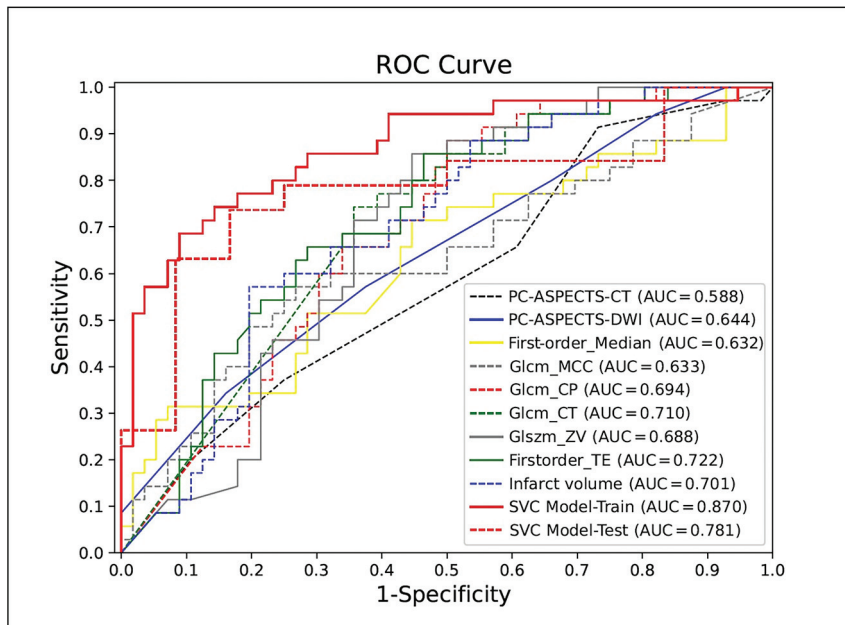


FIG 3. ROC curve results of the best radiomics features from different feature classifications compared with ASPECTS from conventional imaging. PC indicates posterior circulation; CP, cluster prominence; CT, cluster tendency; ZV, zone variance; TE, total energy; ROC, receiver operating characteristic; MCC, maximal correlation coefficient; GLCM, gray level co-occurrence matrix; GLSZM, gray level size zone matrix; SVC, support vector classifier.

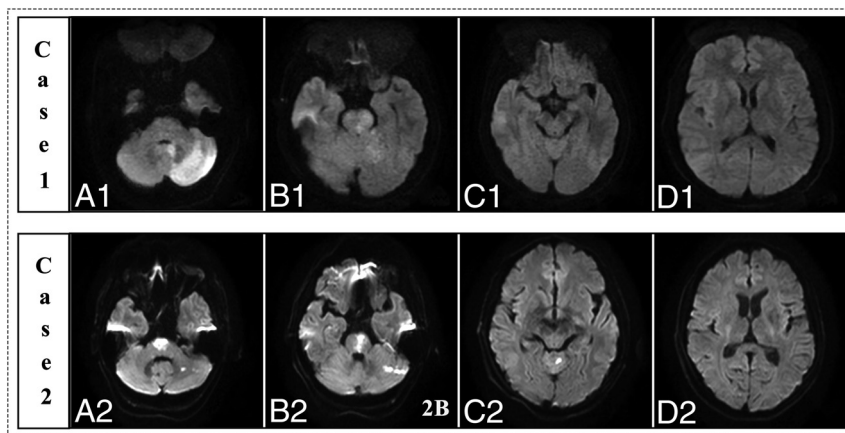


FIG 4. Examples of segmentations from patients with ABAO with favorable (case 2) and unfavorable outcomes (case 1).

Table 2: Diagnostic performance of the radiomics model in the training and testing cohorts

	AUC (95% CI)	Accuracy	Sensitivity	Specificity	PPV	NPV
Training cohort	0.870 (0.784–0.932)	80.4%	82.9%	71.4%	64.5%	86.9%
Testing cohort	0.781 (0.596–0.908)	77.4%	78.9%	75%	83.3%	69.2%

Note:—NPV indicates negative predictive value; PPV, positive predictive value.

weighed when deciding on transport for patients who have received IV thrombolysis or who are imaged at primary hospitals and awaiting transport to comprehensive hospitals.

Currently, there is no established and specific imaging method for preoperative screening of patients with ABAO suitable for EVT. Pc-ASPECTS is a 10-point score widely used in clinical practice to evaluate early ischemic changes. Recently, it has been reported that patients with ABAO with a CT pc-ASPECTS of ≥ 5 benefit from EVT.²² However, it has also been discovered that patients with a higher CT pc-ASPECTS still show significant differences in functional outcomes, with only 11.2% of these patients showing functional independence at 90 days. The posterior fossa radiologic particularities and the anatomic differences in the posterior circulation tend to produce bony artifacts and partial volume effects that reduce its sensitivity and diagnostic accuracy.²³⁻²⁵ Parenchymal changes in the ischemic region may be more easily detected on MR imaging than on CT.²⁶ However, the current research on this aspect is controversial.^{27,28} The possible reasons are that the borderline mRS is different and the assessment method of pc-ASPECTS itself is flawed.

Further calculation of the ischemic degree in the infarct regions and not just the infarct site may be more valuable in evaluating prognosis. Recently, Broocks et al²⁹ created a new imaging score called PCASCO, which combines the collateral circulation status and pc-ASPECTS to predict the prognosis of ABAO stroke. Sun et al³⁰ and Cereda et al³¹ used the critical area perfusion score (CAPS) to quantify serious hypoperfusion (time-to-maximum > 10) in the thalamus and/or midbrain (2 points), pons (2 points), and cerebellum (1 point/hemisphere). Regardless of recanalization, a CAPS of ≤ 3 is a strong independent predictor of a favorable prognosis. The CAPS reweights the infarct region and increases the prognostic value of these imaging markers by adding perfusion information. The CAPS and other scales that consider the topography of the brain are easily accessible and generalizable in the clinical setting and are the cornerstone of diagnostic imaging. RFs can quantitatively describe the spatial relationship of voxels with different gray-scale values within the infarcted region. Driven by the increasing availability of medical data and rapid advances in analytics, RF-based predictive models may provide a new pattern for medical diagnosis and treatment.

Cho et al³² selected 3 typical DWI sections of the brainstem and scored ABAO according to these new slices. Li et al³³ found that the maximum length multiplied by thickness in the brainstem may be a predictor for assessing neurologic deterioration. Consistent with our findings, Liu et al³⁴ and Tajima et al³⁵ found significantly reduced infarct volumes from the midbrain and pons and that increased caudate volumes had favorable clinical outcomes in patients after EVT. Mourand et al³⁶ showed that pre-EVT cerebellar infarct volume was an independent predictor of 90-day functional independence. Because the spatial distribution of nuclear masses in the brain tissue is multilevel,³⁷ using a single level in each brain region may not be sufficient to indicate the severity of the infarct region. Meanwhile, we found that RFs provide quantitative information at each plane and zone and highlight essential brain regions in evaluating the extent of damage more comprehensively.

RFs³⁸ are calculated in a high-dimensional feature space that is transformed from imaging information using massive data-characterization algorithms. These subtle changes, which are difficult to detect by the human eye, are captured by radiologic features in the brain tissue environment. After we analyzed the RFs, the features of predictive value were extracted from the brainstem infarct region. The occipital cortex, thalamus, and cerebellum lesions are less involved in functional outcome than those in the brainstem.³⁵ The numerous key conduction systems that maintain consciousness and physiologic activities cross the brainstem.³⁷ This may explain the worse clinical outcome of infarcts in the brainstem region. Moreover, our algorithm provides quantitative information on RFs, which reduces the interference of human measurements and demonstrates the generalizability of the model on an independent testing set. These findings may help neurologists in the prognosis of patients with ABAO in the EVT era.

Our study has several limitations. First, the small sample size in this study demands a cautious interpretation of the findings and limits the generalization of our results. Future studies should be performed with a larger sample size to better draw clinical inferences. Second, the imaging information used in our study was collected from imaging facilities at multiple centers, resulting in various MR imaging acquisition parameters. The use of multi-vendor images for artificial intelligence algorithms is advocated.³⁹ In our view, radiomics-based models predicting the prognosis of ABAO can be further optimized with much better standardization of imaging data protocols. Third, after acquiring the patient's imaging information, this technique can be used by a neuroradiologist or neurologists. Manual processing of the images takes approximately 20 minutes. The manual segmentation of the ROI on DWI is inefficient in an emergency surgery setting, and future research will have to demonstrate whether this prediction can be performed using automated algorithms. Currently, the software and time required to make predictions are not suitable for clinical applications. Further research in artificial intelligence software may help obtain accurate predictions more quickly.

CONCLUSIONS

The extraction of RFs from the infarct region visualized on preoperative DWI provides information on the prognosis of EVT in patients with ABAO. Characterizing the infarct region, the target of EVT, by radiomics might be a technique that is worth developing to personalize the EVT of patients with ABAO.

Disclosure forms provided by the authors are available with the full text and PDF of this article at www.ajnr.org.

REFERENCES

1. Mattle HP, Arnold M, Lindsberg PJ, et al. **Basilar artery occlusion.** *Lancet Neurol* 2011;10:1002–14 [CrossRef Medline](#)
2. Schonewille WJ, Wijman CA, Michel P, et al. **Treatment and outcomes of acute basilar artery occlusion in the Basilar Artery International Cooperation Study (BASICS): a prospective registry study.** *Lancet Neurol* 2009;8:724–30 [CrossRef Medline](#)
3. Liu X, Xu G, Liu Y, et al. **Acute basilar artery occlusion: Endovascular Interventions versus Standard Medical Treatment (BEST) trial: design and protocol for a randomized, controlled, multicenter study.** *Int J Stroke* 2017;12:779–85 [CrossRef Medline](#)

4. Li C, Wu C, Wu L, et al; BAOCHÉ Investigators. **Basilar Artery Occlusion Chinese Endovascular Trial: protocol for a prospective randomized controlled study.** *Int J Stroke* 2022;17:694–97 [CrossRef Medline](#)
5. Tao C, Li R, Zhu Y, et al. **Endovascular treatment for acute basilar artery occlusion: a multicenter randomized controlled trial (ATTENTION).** *Int J Stroke* 2022;17:815–19 [CrossRef Medline](#)
6. Zi W, Qiu Z, Wu D, et al; Writing Group for the BASILAR Group. **Assessment of endovascular treatment for acute basilar artery occlusion via a nationwide prospective registry.** *JAMA Neurol* 2020;77:561–73 [CrossRef Medline](#)
7. Feng R, Badgeley M, Mocco J, et al. **Deep learning guided stroke management: a review of clinical applications.** *J Neurointerv Surg* 2018;10:358–62 [CrossRef Medline](#)
8. Gillies RJ, Kinahan PE, Hricak H. **Radiomics: images are more than pictures, they are data.** *Radiology* 2016;278:563–77 [CrossRef Medline](#)
9. Kim JY, Park JE, Jo Y, et al. **Incorporating diffusion- and perfusion-weighted MRI into a radiomics model improves diagnostic performance for pseudoprogression in glioblastoma patients.** *Neuro Oncol* 2019;21:404–14 [CrossRef Medline](#)
10. Zhang YQ, Liu AF, Man FY, et al. **MRI radiomic features-based machine learning approach to classify ischemic stroke onset time.** *J Neurol* 2022;269:350–60 [CrossRef Medline](#)
11. Quan G, Ban R, Ren JL, et al. **FLAIR and ADC image-based radiomics features as predictive biomarkers of unfavorable outcome in patients with acute ischemic stroke.** *Front Neurosci* 2021;15:730879 [CrossRef Medline](#)
12. Wang H, Sun Y, Ge Y, et al. **A clinical-radiomics nomogram for functional outcome predictions in ischemic stroke.** *Neurol Ther* 2021;10:819–32 [CrossRef Medline](#)
13. Hofmeister J, Bernava G, Rosi A, et al. **Clot-based radiomics predict a mechanical thrombectomy strategy for successful recanalization in acute ischemic stroke.** *Stroke* 2020;51:2488–94 [CrossRef Medline](#)
14. Chen X, Li Y, Zhou Y, et al. **CT-based radiomics for differentiating intracranial contrast extravasation from intraparenchymal haemorrhage after mechanical thrombectomy.** *Eur Radiol* 2022;32:4771–79 [CrossRef Medline](#)
15. Qiu W, Kuang H, Nair J, et al. **Radiomics-based intracranial thrombus features on CT and CTA predict recanalization with intravenous alteplase in patients with acute ischemic stroke.** *AJNR Am J Neuroradiol* 2019;40:39–44 [CrossRef Medline](#)
16. Fedorov A, Beichel R, Kalpathy-Cramer J, et al. **3D Slicer as an image computing platform for the Quantitative Imaging Network.** *Magn Reson Imaging* 2012;30:1323–41 [CrossRef Medline](#)
17. Puetz V, Sylaja PN, Coutts SB, et al. **Extent of hypoattenuation on CT angiography source images predicts functional outcome in patients with basilar artery occlusion.** *Stroke* 2008;39:2485–90 [CrossRef Medline](#)
18. Koo TK, Li MY. **A guideline of selecting and reporting intraclass correlation coefficients for reliability research.** *J Chiropr Med* 2016;15:155–63 [CrossRef Medline](#)
19. Liu J, Tao W, Wang Z, et al. **Radiomics-based prediction of hemorrhage expansion among patients with thrombolysis/thrombectomy related-hemorrhagic transformation using machine learning.** *Ther Adv Neurol Disord* 2021;14:17562864211060029 [CrossRef Medline](#)
20. Hui FK, Obuchowski NA, John S, et al. **ASPECTS discrepancies between CT and MR imaging: analysis and implications for triage protocols in acute ischemic stroke.** *J Neurointerv Surg* 2017;9:240–43 [CrossRef Medline](#)
21. Knip HC, Elsayed S, Nawabi J, et al. **Imaging-based outcome prediction in posterior circulation stroke.** *J Neurol* 2022;269:3800–09 [CrossRef Medline](#)
22. Sang H, Li F, Yuan J, et al. **Values of baseline posterior circulation acute stroke prognosis early computed tomography score for treatment decision of acute basilar artery occlusion.** *Stroke* 2021;52:811–20 [CrossRef Medline](#)
23. Pallesen LP, Khomenko A, Dzialowski I, et al. **CT-angiography source images indicate less fatal outcome despite coma of patients in the Basilar Artery International Cooperation Study.** *Int J Stroke* 2017;12:145–51 [CrossRef Medline](#)
24. Ravindren J, Aguilar Perez M, Hellstern V, et al. **Predictors of outcome after endovascular thrombectomy in acute basilar artery occlusion and the 6hr time window to recanalization.** *Front Neurol* 2019;10:923 [CrossRef Medline](#)
25. Hwang DY, Silva GS, Furie KL, et al. **Comparative sensitivity of computed tomography vs. magnetic resonance imaging for detecting acute posterior fossa infarct.** *J Emerg Med* 2012;42:559–65 [CrossRef Medline](#)
26. Warach S, Chien D, Li W, et al. **Fast magnetic resonance diffusion-weighted imaging of acute human stroke.** *Neurology* 1992;42:1717–23 [CrossRef Medline](#)
27. Yang H, Ma N, Liu L, et al. **Early diffusion-weighted imaging brain stem score for acute basilar artery occlusion treated with mechanical thrombectomy.** *J Stroke Cerebrovasc Dis* 2018;27:2822–28 [CrossRef Medline](#)
28. Yoon W, Kim SK, Heo TW, et al. **Predictors of good outcome after stent-retriever thrombectomy in acute basilar artery occlusion.** *Stroke* 2015;46:2972–75 [CrossRef Medline](#)
29. Brooks G, Meyer L, Faizy TD, et al. **New imaging score for outcome prediction in basilar artery occlusion stroke.** *Eur Radiol* 2022;32:4491–99 [CrossRef Medline](#)
30. Sun D, Huo X, Raynald, et al. **Outcome prediction value of critical area perfusion score for acute basilar artery occlusion.** *Interv Neuroradiol* 2022 Sep 13. [Epub ahead of print] [CrossRef Medline](#)
31. Cereda CW, Bianco G, Mlynash M, et al. **Perfusion imaging predicts favorable outcomes after basilar artery thrombectomy.** *Ann Neurol* 2022;91:23–32 [CrossRef Medline](#)
32. Cho TH, Nighoghossian N, Tahon F, et al. **Brain stem diffusion-weighted imaging lesion score: a potential marker of outcome in acute basilar artery occlusion.** *AJNR Am J Neuroradiol* 2009;30:194–98 [CrossRef Medline](#)
33. Li H, Dai Y, Wu H, et al. **Predictors of early neurologic deterioration in acute pontine infarction.** *Stroke* 2020;51:637–40 [CrossRef Medline](#)
34. Liu C, Song JX, Guo ZB, et al. **Prognostic structural neural markers of MRI in response to mechanical thrombectomy for basilar artery occlusion.** *Front Neurol* 2021;12:593914 [CrossRef Medline](#)
35. Tajima Y, Hayasaka M, Ebihara K, et al. **Predictors of very poor outcome after mechanical thrombectomy for acute basilar artery occlusion.** *Neurol Med Chir (Tokyo)* 2020;60:507–13 [CrossRef Medline](#)
36. Mourand I, Mahmoudi M, Dargazanli C, et al. **DWI cerebellar infarct volume as predictor of outcomes after endovascular treatment of acute basilar artery occlusion.** *J Neurointerv Surg* 2021;13:995–1001 [CrossRef Medline](#)
37. Sciacca S, Lynch J, Davagnanam I, et al. **Midbrain, pons, and medulla: anatomy and syndromes.** *Radiographics* 2019;39:1110–25 [CrossRef Medline](#)
38. Sarioglu O, Sarioglu FC, Capar AE, et al. **Clot-based radiomics features predict first pass effect in acute ischemic stroke.** *Interv Neuroradiol* 2022;28:160–68 [CrossRef Medline](#)
39. Bluemke DA, Moy L, Bredella MA, et al. **Assessing radiology research on artificial intelligence: a brief guide for authors, reviewers, and readers—From the Radiology Editorial Board.** *Radiology* 2020;294:487–89 [CrossRef Medline](#)